IEEE Access
Multidisciplinary | Rapid Review | Open Access Journal

Received September 6, 2019, accepted September 22, 2019, date of publication October 3, 2019, date of current version October 16, 2019.

Digital Object Identifier 10.1109/ACCESS.2019.2945483

Load Guided Signal-Based Two-Stage Charging Coordination of Plug-In Electric Vehicles for Smart Buildings

SEUNGWOOK YOON, (Student Member, IEEE), AND EUISEOK HWANG, (Member, IEEE)
School of Mechatronics, Gwangju Institute of Science and Technology, Gwangju 61005, South Korea

Corresponding author: Euiseok Hwang (euiseokh@gist.ac.kr)

This work was supported in part by the Korea Institute of Energy Technology Evaluation and Planning (KETEP) and the Ministry of Trade, Industry and Energy (MOTIE) of South Korea under Grant 20171210200810, and in part by the Gwangju Institute of Science and Technology (GIST) Research Institute (GRI) Grant funded by GIST in 2019.

ABSTRACT A novel plug-in electric vehicle (PEV) charging coordination scheme for smart buildings, processed in two separate stages bridged by a load guided signal, is proposed in this study. The goal of the proposed coordination is to minimize the overall energy cost of the building, while satisfying the desired target and operation range of the state of charge (SoC) of each PEV. As the PEV penetration level grows, uncoordinated charging may impact the stability of the building's energy system by increasing the peak demand and introducing uncertainty. Consequently, the charging decisions on the PEV fleet require considering the uncertainty of the drivers' behavior and the power demand pattern of the coupled building. In this study, a customized load guided signal is introduced for PEV fleet charging. It formulated and implemented through mixed integer linear programming in two separate stages. The first stage involves the extraction of the electric vehicle supply equipment (EVSE) based guide signal for the benefits and physical constraints of the building's energy system. The load guided signals are created by jointly investigating the charging/discharging flexibility of the EVSE using load prediction and the PEV fleet to minimize the electricity cost in the time-of-use energy market. In the second stage, the priority weight is exploited for distributing the charging/discharging decisions for individual PEVs. To evaluate the performance of the proposed method, numerical evaluations were conducted at various PEV penetration levels using a pair of energy consumption and vehicle parking datasets for the building. The case study demonstrates that the proposed scheme provides 12% load factor improvement and 13% cost reduction at a 50% PEV penetration level.

INDEX TERMS Plug-in electric vehicles (PEVs), vehicle-to-grid (V2G), economic charging strategies, charge scheduling, demand response.

NOMENCLATURE

INDICES

i Index of the plug-in electric vehicle (PEV), $i \in \{1, 2, ..., I\}$.

k Index of the electric vehicle supply equipment (EVSE), $k \in \{1, 2, ..., N^{ch}\}$.

t Index of time slot, $t \in \{1, 2, ..., T\}$.

PARAMETERS AND CONSTANTS

γ^{ch}	Charging rate of the multi-charger station (kW).
γ^{dch}	Discharging rate of the multi-charger station (kW).
η^{ch}	Charging efficiency of the multi-charger station.
η^{dch}	Discharging efficiency of the multi-charger station.
B_i	Battery capacity of the i^{th} PEV (kWh).
ψ_i^{max}	Maximum allowed battery capacity range of the i^{th} PEV (kWh).
ψ_i^{min}	Minimum allowed battery capacity range of the i^{th} PEV (kWh).
t_i^{dep}	Departure time slot of the i^{th} PEV.

The associate editor coordinating the review of this manuscript and approving it for publication was Yunfeng Wen.

t_i^{arr}	Arrival time slot of the i^{th} PEV.
ξ_t^{ch}	Price per kWh of electricity for purchasing from the grid at the t^{th} time slot (KRW/kWh).
ξ_t^{dch}	Price per kWh of electricity for selling the electricity at the t^{th} time slot (KRW/kWh).
P^{ct}	Contracted power of the building.
c^B	Demand cost per kW of the building (KRW/kW).
N^{ch}	The number of the available EVSEs in the PEV charging station.
N_t^{PEV}	The number of PEVs in PEV charging station at the t^{th} time slot.
κ	The duration of the unit time slot.
χ^{deg}	The battery degradation cost when the EVSE charges a PEV or discharges from a PEV in the unit time slot (KRW).
β	The battery cost of a PEV (KRW/kWh).
l	The cycle life of the PEV battery.
α	The state-of-charge (SoC) level for the control of battery management.

VARIABLES

P_t^B	Building power without PEVs at the t^{th} time slot in kW.
$\hat{P}_t^B$	Predicted building power without PEVs at the t^{th} time slot in kW.
C_{fc}	Facility-related demand cost (KRW).
C_{ToU}	Price for purchasing/selling electricity based on ToU tariffs (KRW).
C_{ip}	Incentive/penalty based cost (KRW).
C_{deg}	Battery degradation cost based on the k^{th} EVSE (KRW).
$e\delta_{k,t}^{ch}$, $e\delta_{k,t}^{dch}$	Charging and discharging indicators of the k^{th} EVSE, $e\delta_{k,t}^{ch}, e\delta_{k,t}^{dch} \in \{0, 1\}$.
$p\delta_{i,t}^{ch}$, $p\delta_{i,t}^{dch}$	Charging and discharging indicators of the i^{th} PEV, $p\delta_{i,t}^{ch}, p\delta_{i,t}^{dch} \in \{0, 1\}$.
ψ_i^{ini}	Initial SoC for the i^{th} PEV.
ψ_j^{dep}	Departing SoC for the i^{th} PEV.
λ_t^i	The probability density function for the existence of the i^{th} PEV. b_t^i The weight for the battery management of the i^{th} PEV.

I. INTRODUCTION

Incresing environment concerns and fossil-fuels exhaustion are boosting plug-in electric vehicles (PEVs) as a practical solution for sustainable transportation. The PEV market increased sharply over the past decades as additional supports emerge in countries with the global PEV stock expected to reach 20 million in 2020 [1]. However, large-scale adoption of PEVs increases the peak electricity demand, requiring extra power plants, and degrades the stability of the power system on the building's energy system [2]. Furthermore, the uncertainty of PEV charging, if uncoordinated, causes several undesired side effects including voltage drop, power loss, and high energy cost [3], [4]. Contrarily, PEVs provide numerous grid services like cost minimization, peak power reduction [5], valley filling [6], [7], and voltage management [8] by exploiting the battery of the PEV as a distributed energy resource (DER) with bi-directional charging. Besides, since the idle time of most vehicles takes about 90% of a regular day in the parking lot [9], PEV charging time is widely shiftable and is flexible [10].

Smart integration of a PEV or PEV fleet to a building energy system involves studies with broad perspectives including bi-directional charging capability supporting vehicle-to-grid (V2G) and conventional grid-to-vehicle (G2V) [11]. Several potential grid services associated with PEVs have been investigated in recent years [12]. Operation modes like G2V and V2G enhance the reliability of the power system and reduce energy costs by properly selling and purchasing power. The PEV charging coordination for reducing energy costs is investigated in [13]. In [13], the PEV battery reaches the desired state-of-charge (SoC), followed by the PEV owner incentive cost with adjustment of the charging schedule during the time left. The application of PEV charging schemes in vehicle-to-building (V2B) systems require satisfaction of the PEV owner for driving since the driving pattern is critical from the vehicle's perspective.

Consequently, many researchers have studied driving patterns and modeled the PEV battery. In [14], six driving patterns of vehicles were modeled using fuzzy modeling, with the PEV charging scheduling method implemented based on the driving pattern models. Likewise, reference [15] analyzed the distribution of the traveling distance of PEVs and the energy level of the battery using historical PEV driving data. However, the uncertainty of PEV mobility and fairness assignment of the charging amount were neglected in these studies. Since it is unreasonable to use a battery of a particular PEV frequently due to battery degradation, the coordinator of the PEV management system must allocate charging/discharging schedules between PEVs fairly. In [16], a fairness energy scheduling algorithm is proposed by evaluating the charging priority of each PEV. In a residential energy system, fair charging and discharging between PEVs is performed to reduce peak power. Moreover, reference [17] evaluates the charging priority to mitigate charging service conflicts and reduce the energy cost in the office environment.

The price of a PEV is currently higher than that of a fossil-fuel vehicle because of the battery cost [18]. Thus, the additional cost benefits to the PEV's owner are needed to increase the PEV market. Although PEV fleets provide a variety of services, typical consumers including PEV and building owners desire control of the electric devices for reduction of the energy cost. Therefore, electric utilities manage the power demand of the PEV fleet by appropriately adjusting the price-signal, because the general PEV charging scheme is dependent on the price-signal. The price-signal is divided into the energy cost, demand cost and incentive/penalty-based rate like demand response (DR) [19]. The positive economic effect of V2G is reported in [20], [21], with optimal charging strategies for energy reduction investigated by many research

groups. In [22], the PEV charging operations of a PEV fleet in a charging station was evaluated in the diverse electricity market including the time of use (ToU), real time price (RTP) and DR. In [23], a PEV charging strategy is proposed for minimizing the energy cost by restraining the increases in facility-related demand cost by a PEV fleet through the reduction of maximum peak load in the ToU market. In [24], a charging coordination scheme is advanced for maximizing the profit while mitigating potential overloads and minimizing the cost to PEV owners, considering the RTP/DR market. Similarly, reference [25] evaluates the RTP and DR based charging strategies using the PEV and energy storage system (ESS) in residential building. In [26], the distributed DR algorithm is proposed to maximize the benefit to the PEV owner in the DR market, with the convenience evaluated.

To control a large-scale PEV fleet, the PEV charging coordination method necessitates various considerations like uncertainty of the PEV owners' behavior, the battery charging cost, and the energy state of the parking station. Many researchers therefore investigated multi-level optimization methods. In [27], a bi-level coordination model is proposed, with the upper-level optimization model enabling profit maximization for the aggregation of the power system, while the lower-level optimization model provides profit for the parking station. Reference [28] suggests a bi-level PEV coordination model, where the first-level optimization maximizes the benefits to the PEV owner through the PEV characteristics and the second-level optimization ensures the minimization of the system cost. Reference [29] utilized a two-stage optimization method for power management comprising a first-level optimization for active power management and a second-level for reactive power management.

This study proposes an effective PEV charging coordination method that minimizes the energy cost while maximizing the PEVs' owners satisfaction by considering the electrical equipment of the smart building. To meet these perspectives, this study employs a two-stage optimization. In the first-stage optimization, the load shape of the building for minimization of the energy cost through the EVSEs' charging operations is handled. The energy profile based on the EVSEs in the PEV charging station is defined as the load guided signal for charging/discharging controls of PEVs. The load guided signal is created by jointly investigating the price-signal, load profile of the building, and energy flexibility of the PEV charging station. Thereafter, the second-stage optimization coordinates the charging schedule of each PEV to satisfy the desired SoC of each PEV and the load guided signal. This two-stage optimization problem is formulated in the day-ahead scenario as a mixed integer linear programming problem. The proposed model considers the uncertainty of the PEV owners' behaviors, and the prediction error related to the building load. Although minimization of the energy cost and the behavior of PEVs have been intensively studied, no previous work evaluates the flexibility of EVSEs in the PEV charging station and handles fairness of the charging amount with the uncertainty of PEV owners behaviors. Hence, the contribution of this study is summarized as follows:

- Development of a two-stage optimization model to minimize energy cost and improve the stability of the building's energy system
- To model a realistic PEV charging coordination scheme, calculation of energy flexibility on a PEV parking station based on evaluation of the available energy of EVSEs
- Fair assignment of the charging amount between PEVs considering the uncertainty of PEV owners' behaviors

A system model is introduced for the proposed scheme in Section II, while the load guided signal based the two-stage charging coordination is described in Sections III-IV. Case studies are presented in Section V, and Section VI contains conclusions.

II. SYSTEM MODEL

The operation of the scheme proposed in this study illustrated in Fig. 1. The proposed system minimizes the energy cost by controlling electric components in a building energy system. The energy management system acquires information on parameters like the SoC levels of the PEV fleet, the predicted building load, and the charging/discharging prices of the EVSEs. The data are transferred using communication methods including zigbee and WIMAX [30]. The integrity of communication is assumed in the proposed model. The proposed algorithm uses data for various parameters to initiate charging of EVSEs as needed, saving energy cost while serving the desired battery levels of the PEV fleet. The components of the system model are described in subsequent sections.

A. THE PEV MOBILITY MODEL

To explain the method proposed in Section III, the mobility of the PEV fleet is an important factor since it determines the available energy supporting the building's energy system. Thus, the departure/arrival times of the PEV fleet must be decided before applying the proposed algorithm. Modeling of the mobility of the PEV fleet requires the vehicle in-and-out data of parking management system, and that provided by the C research institute in South Korea is used. The mobility models rely on Gaussian distributions through K-means clustering in Fig. 2 [23]. The PEV fleet model is defined as three types including the full day (F), morning (M), and afternoon (A) based on arrival times (t_i^{arr}) and the parking duration (d_i) of the PEV fleet. Since C building is a commercial-type building, the F type represents the general mobility model of workers and is modeled through the bivariate normal distribution $(d_F, t_F) \sim \mathcal{N}(\mu_F, \Sigma_F)$. Likewise, M and A types in Fig. 2 are driving patterns of visitors modeled through bivariate log-normal distribution like $(ln(d_M), ln(t_M^{arr})) \sim \mathcal{N}(\mu_M, \Sigma_M)$ and $(ln(d_A), ln(t_A^{arr})) \sim \mathcal{N}(\mu_A, \Sigma_A)$.

B. THE PEV BATTERY MODEL

The amount of flexible energy of the PEV fleet for various grid services depends on the capacity of the PEV battery

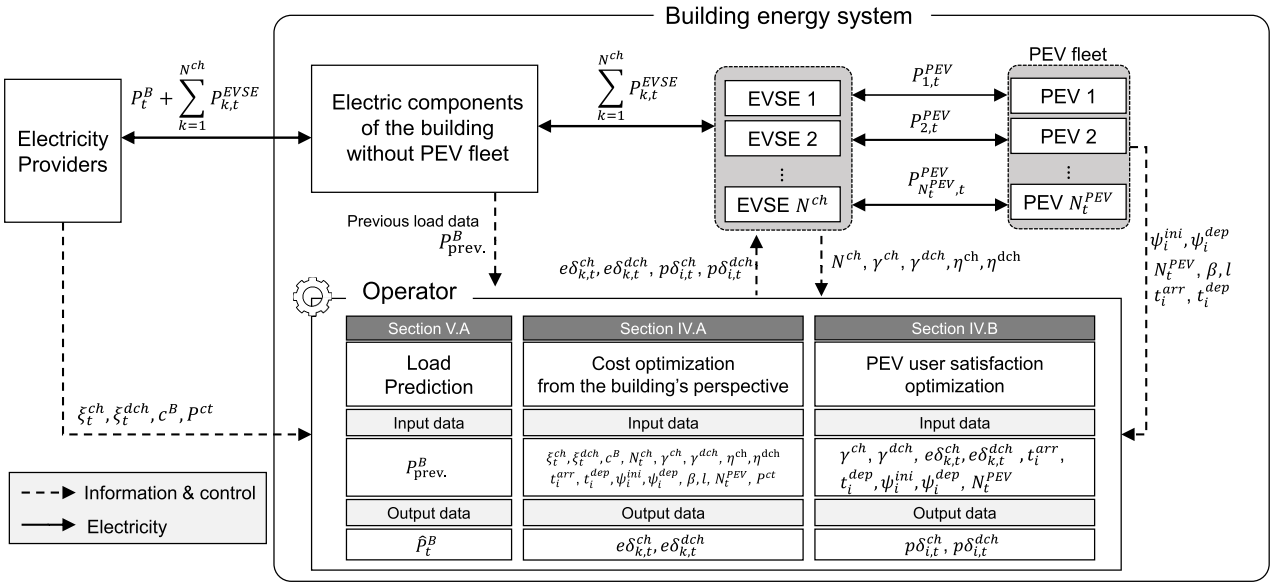

FIGURE 1. Overall flow of the proposed system based on two-stage optimization.

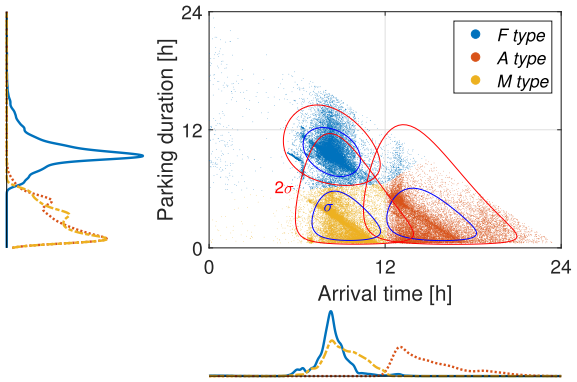

FIGURE 2. Vehicle fleet pattern modeling from the C research institute data.

and the arrival/departure SoCs. To simulate the proposed algorithm, PEV models with three efficiencies ϵ and battery capacities B are considered (Table 1). Furthermore, the daily driving distance is modeled as $D \sim \mathcal{N}(\mu_d, \Sigma_d)$, where μ_d and Σ_d are the mean and standard deviation of the driving distance of the statistical driving data from South Korea [31]. In addition, the arrival/departure SoCs of the PEV fleet are formulated using the daily driving distance given by

$$\psi_i^{ini} = \psi_i^{min} + \phi_i, \quad \psi_i^{dep} = \frac{D}{2\epsilon} + \psi_i^{ini}, \tag{1}$$

where ϕ_i is a random value based on the normal distribution for the initial SoC, that expresses the uncertainties of the arrival times depending on the driving patterns of PEV owners. In addition, D assumes the driving distance on the round trip, whereas ψ_i^{dep} considers only a one-way trip. To test more realistic scenarios, the battery stress model based on the EVSE, χ^{deg}, should also be exploited, indicating the

TABLE 1. Specifications of PEVs.

Vehicle model	Battery, B capacity [kWh]	Driving efficiency, ϵ [km/kWh]
2018 Niro EV	64	5.3
2018 IONIQ	28	6.3
2018 Soul EV	30	5.2

battery cost when the k-th EVSE charges any PEV in one-time slot. The battery lifetime depends on the battery usage pattern of the PEV's owner, and it is quiet variable [32]. Hence, the battery stress model based on the charging rates of EVSEs is evaluated by considering the battery lifetime given below as

$$\chi^{deg} = \frac{\kappa \times \gamma^{ch} \times \beta}{2 \times l} \quad [\text{KRW}], \tag{2}$$

where β and l are the battery cost per kWh and the cycle life of battery, respectively, and κ is the duration of the one-time slot, e.g., 15 min.

C. CHARGING STATION MODEL

The PEV charging station model for the smart building involves constant charging/discharging rates including a slow or fast charger. Thus, the two EVSE models involved include:

(1) Slow EVSE model: the slow EVSE involves charging/discharging rates between 3 and 6kW, with the full PEV recharging generally taking 4 to 12 hours. The efficiency of the charging/discharging operation is higher than that of the fast charger.
(2) Fast EVSE model: fast chargers involve charging/discharging rates between 7 and 22kW. The fast

TABLE 2. Energy tariff for general service for the building load.

Demand cost (KRW/kW)	Energy cost (KRW/kWh)			
	Time slot	Summer	Spring/Fall	Winter
7,170	Off-peak load	62.7	62.7	71.4
	Mid-load	113.9	70.1	101.8
	Peak-load	136.4	81.4	116.6

TABLE 3. Energy tariff for electric vehicle charging.

Demand cost (KRW/kW)	Energy cost (KRW/kWh)			
	Time slot	Summer	Spring/Fall	Winter
2,580	Off-peak load	52.5	53.5	69.9
	Mid-load	110.7	64.3	101.0
	Peak-load	163.7	68.2	138.8

TABLE 4. Time slot for each season.

Time	Summer	Spring/Fall	Winter
	(Time slot (hour))		
Off-peak load	23-09	23-09	23-09
Mid-load	09-10	09-10	09-10
	12-13	12-13	12-17
	17-23	17-23	20-22
Peak-load	10-12	10-12	10-12
	13-17	13-17	17-20
			22-23

EVSE generates high load instantaneously or vice versa in the building's energy system.

To apply the PEV charging coordination scheme, the energy demand of each EVSE is expressed using the charging/discharging rates given below as

$$P_{k,t}^{EVSE} = \gamma^{ch}\eta^{ch}e\delta_{k,t}^{ch} + \gamma^{dch}\eta^{dch}e\delta_{k,t}^{dch}, \tag{3}$$

with constraints

$$e\delta_{k,t}^{ch} + e\delta_{k,t}^{dch} \leq 1 \tag{4}$$

The charging and discharging operations of PEVs involves losses like transformer loss in the building, energy conversion losses of the EVSE and PEVs, and transmission loss. If charging/discharging operations are controlled using nominal power rates without considering losses, the desired SoC level of each PEV may be unsatisfied or the building energy may become more unstable. Therefore, the efficiencies of EVSEs are considered with the charging/discharging rates. The charging/discharging rates of the PEVs assume constant values, γ_k^{ch} and γ_k^{dch}, whereas the charging/discharging rates of the building consider the loss between batteries of PEVs and the transformer of the building. To deliver the desired charging energy to the PEV, the transfer of the charging energy including the energy losses is required. Contrarily, the energy received at the building is lower than the discharging energy of the PEV because of the energy losses. Thus, η_k^{ch} is greater than 1 while η_k^{dch} is lesser than 1.

D. PRICE DATA

The electricity market price modeling is based on the general services ToU energy tariff model and the PEV charging services ToU tariff model from Korea electric power corporation described in Table 2 and Table 3, respectively. The energy tariff for general services implies the price information of the grid providing the building with electricity. Since the two energy tariffs are different, building operators can choose an electricity seller including the grid and PEV owners by comparing the price information. Also, South Korea's ToU tariffs change each season as shown in Table 4 [17]. The PEV owners and building operators coordinate to purchase or sell energy by referring to Table 4 to minimize energy costs.

In addition to the ToU tariff, baseline costs based on demand cost linearly dependent on the contracted power and a 2.5 times penalty for excessive usage over the contract also exist. Thus, the baseline cost is reduced by lowering the contracted power, whereas the overall cost is increased by frequent penalties of excess power utilization. Therefore, the contracted power requires careful determination by jointly analyzing the building load and the PEV charging/discharging behaviors.

III. PROBLEM STATEMENT

The proposed methodology for optimizing the PEV charging coordination described in this section is summarized in Fig. 3. The building comprises electric components including PEVs, workloads, and DERs. Arbitrary activation of such components may degrade the stability of the building's energy system because the behaviors of users involve sufficient randomness. To mitigate the impact on the stability of the energy system while minimizing the electricity cost, the actions of the controllable components are carefully adjusted by considering randomness and uncertainties. This paper therefore proposes a two-stage optimization method for the efficient management of energy by coordination of the charging of PEVs in smart buildings. In general, individual PEV owner's desire the cost benefit maximization by controlling the charging/discharging operation of batteries. However, the limited electrical resources of the building is unable to accommodate all requirements of PEVs, and the high energy demands of a PEV fleet is generated in a low-price timezone in [17]. Therefore, energy flexibility is defined by jointly evaluating the electrical equipment of the building and the price information. Given the energy flexibility of the building, the charging decision of the EVSE is favorably coordinated for stabilization of the building's energy system. Also, centralized optimization is required to incorporate all physical and cost conditions. That is, the PEV owners provide their charging control to the building operator, and the building operator satisfies the customer charging demands, while minimizing the electricity cost. This study assumes that the building operator pays the usage fees for the extra battery usage of PEVs.

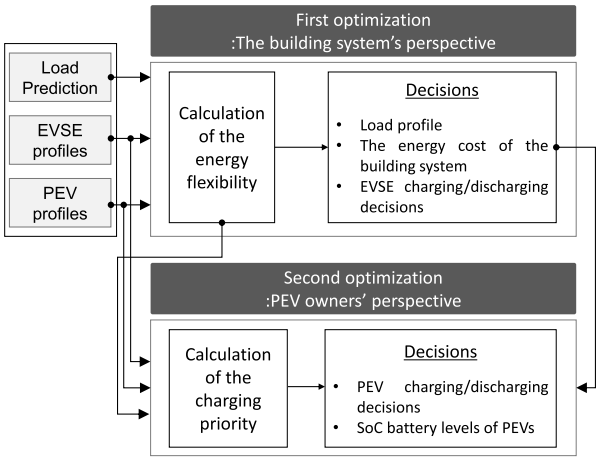

FIGURE 3. The proposed two-stage PEV charging coordination method.

IV. MATHEMATICAL MODEL

A. FIRST OPTIMIZATION: BUILDING ENERGY MANAGEMENT

The first optimization finds the charging/discharging operating schedules of EVSE, $e\delta_{k,t}^{ch}$ and $e\delta_{k,t}^{dch}$, that minimizes the overall cost function while considering the physical constraints as below:

$$\min_{e\delta_{k,t}^{ch}, e\delta_{k,t}^{dch}} (C_{ToU} + C_{ip} + C_{fc} + C_{deg}) \tag{5}$$

The overall cost consists of the four terms in Eq. (5) including the electricity costs of charging/discharging in the ToU tariff, the penalty cost based on the contracted power, the baseline cost of the contracted power, and the battery degradation cost, respectively.

1) ELECTRICITY COSTS BASED ON TOU TARIFF

The first term is formulated by considering the charging/discharging operation profiles of the EVSE from the building energy system's perspective as below:

$$C_{ToU} = \sum_{t=1}^{T} \sum_{k=1}^{N^{ch}} \xi_{k,t}^{cost}, \tag{6}$$

where

$$\xi_{k,t}^{cost} = \begin{cases} \xi_t^{ch} \times P_{k,t}^{EVSE}, & P_{k,t}^{EVSE} \geq 0 \\ \xi_t^{dch} \times P_{k,t}^{EVSE}, & P_{k,t}^{EVSE} < 0 \end{cases} \tag{7}$$

The charging/discharging rates of EVSEs, $P_{k,t}^{EVSE}$, in Eq. (3) is adjusted in consideration of the electricity costs by the time based on the ToU tariff to minimize the charging/discharging cost. In the multi-charger station, the number of available EVSEs equals the number of connected PEVs, if all PEVs utilize EVSE.

2) CONTRACTED POWER BASED BASELINE COST

Since the contracted power is changed by evaluating the maximum peak load and the average power demand of the building, reduction of the baseline cost is possible through control of the energy resources. For management of the peak load, the baseline cost of the building is given by

$$C_{fc} = \frac{c^B \times \max(P_t^B + \sum_{k=1}^{N^{ch}} P_{k,t}^{EVSE})}{30\text{days}}, \tag{8}$$

where c^B is the demand cost of the building in Table 2. Since the demand cost for contracted power is paid monthly, the demand charge is divided by 30 to apply the day-ahead scenario.

3) INCENTIVE/PENALTY COST BASED ON THE LOAD PROFILE

The third term in Eq. (5) is formulated by evaluating the excess power, and meaning the additional cost based on the load profile like DR. In South Korea's electricity market of South Korea, the building operator pays the penalty fee when the power demands of a building exceed the contracted power. In the proposed method, the penalty cost considered without the incentive cost, as below:

$$C_{ip} = \begin{cases} \dfrac{2.5 \times c^B \times P^{pty}}{30\text{days}}, & P^{pty} \geq 0 \\ 0, & \text{otherwise}, \end{cases} \tag{9}$$

where

$$P^{pty} = \max(P_t^B + \sum_{k=1}^{N^{ch}} P_{k,t}^{EVSE} - P^{ct}) \tag{10}$$

In Eq. (9), $C_{ip}(t)$ employs the 2.5 times penalty cost for excessive power. Increasing the P^{ct} reduces the penalty fee, but adds the baseline cost in the building.

4) BATTERY DEGRADATION COST

The increase in charging amounts of each PEV incurs battery degradation cost. To reduce the battery degradation cost, the forth term is formulated using Eq. (2), as below:

$$C_{deg} = \chi^{deg} \sum_{t=1}^{T} \sum_{k=1}^{N^{ch}} (e\delta_{k,t}^{ch} + e\delta_{k,t}^{dch}) \tag{11}$$

The battery degradation costs of connected PEVs assume a constant value since it cannot be calculated precisely in real-time.

5) ENERGY FLEXIBILITY OF BUILDING

The available energy capacity of the building is determined by estimating the size of the internal DER capacity in the building. If the DERs share energy in the building, the building energy system is perceived as a unitary energy system. To evaluate the energy flexibility of the building, that of each DER, i.e., PEV and ESS, must be calculated preferentially. The available energy for a PEV each hour, $F_{i,t}^{PEV}$, is calculated using the information of the PEVs' battery including the

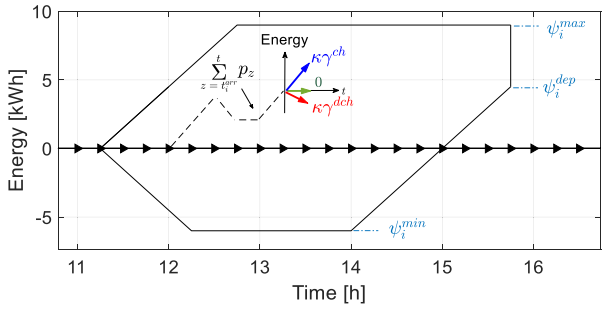

FIGURE 4. The energy flexibility for a PEV.

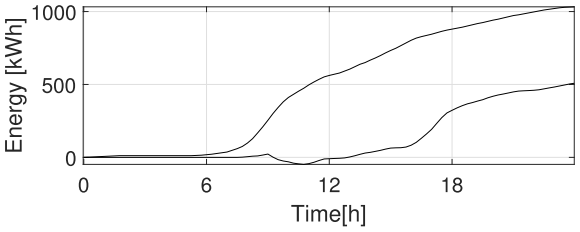

FIGURE 5. The energy flexibility for the building energy system for day-ahead scenario with the PEV penetration level 40%.

initial SoC, departing SoC, and maximum capacity as given below:

$$\begin{aligned} F_{i,t}^{PEV} &= F_{i,t}^1 \cap F_{i,t}^2 \cap F_{i,t}^3 \\ F_{i,t}^1 &= \{(p_t, t) | p_t \in [\kappa\gamma^{dch}, 0, \kappa\gamma^{ch}], t_i^{arr} < t < t_i^{dep}\} \\ F_{i,t}^2 &= \{(p_t, t) | \sum_{t=t_i^{arr}}^{t_i^{dep}} p_t + \psi_i^{ini} > \psi_i^{dep}, t \geq t_i^{dep}\} \\ F_{i,t}^3 &= \{(p_t, t) | \psi_i^{min} < \sum_{z=t_i^{arr}}^{t} p_z + \psi_i^{ini} < \psi_i^{max}\}, \end{aligned} \quad (12)$$

where p_t is controllable energy of a PEV at time t. The $F_{i,t}^1$ is the available energy at time t when the PEV is in the PEV charging station. When the PEV departs the station, the SoC level of the PEV should contain the desired energy in its battery. This constraint is denoted as $F_{i,t}^2$. Also, the $F_{i,t}^3$ limits the charging amounts by considering the maximum and minimum capacity of the PEV's battery, with z as the time index for the cumulative sum. The energy flexibility of the PEV is illustrated in Fig. 4.

For the evaluation of the total available energy of the building at each hour, the information of the PEV charging station is evaluated by jointly combining the energy flexibilities of the PEV fleet. The F_t^{ST} is introduced as the number of the PEVs' charging/discharging operations, which is lower than the number of EVSE and the number of the parked PEVs, and given below as

$$F_t^B = (\cup_{i=1}^{I} F_{i,t}^{PEV}) \cap F_t^{ST}, \quad (13)$$

where

$$F_t^{ST} = \{(e\delta_{k,t}^{ch}, e\delta_{k,t}^{dch}, t) | \sum_{k=1}^{N^{ch}} (e\delta_{k,t}^{dch} + e\delta_{k,t}^{ch}) < \min(N_t^{PEV}, N^{ch})\} \quad (14)$$

Thus, F_t^B expresses the available energy boundaries of the building by exploiting the states of the EVSE and PEVs in the building in Fig. 5. The proposed method controls the charging/discharging operations of the PEV fleet within the F_B to minimize the overall electricity cost, and the charging/discharging operations of EVSE defines the load guided signal for the control of the charging/discharging operations of the PEV fleet.

B. SECOND OPTIMIZATION: PEV USER SATISFACTION

To efficiently control the charging/discharging operations of the PEV fleet, the first optimization method only considers the overall cost of the building, whereas the second optimization method only evaluates the user satisfaction of the PEV. In the first optimization, the load guided signal is generated from the evaluation of the electricity cost, and the charging/discharging operations of the PEVs, $p\delta_{i,t}^{ch}$ and $p\delta_{i,t}^{dch}$, are controlled to satisfy ensure the summation of their charging energies equals the load guided signal in the second optimization. The objective function for energy management of the PEV fleet considers the user satisfaction values, which are defined by using the probability density function of the parked time of the PEV and the weights for battery control and given as below:

$$\min_{p\delta_{i,t}^{ch}, p\delta_{i,t}^{dch}} \sum_{i=1}^{I} \sum_{t=t_i^{arr}}^{t_i^{dep}} (w_1 \lambda_t^i + w_2 b_t^i), \quad (15)$$

where λ_t^i and b_t^i are the probability density functions for the i^{th} PEV's existence in the PEV charging station and the weight for battery management of the i^{th} PEV, respectively. Also, w_1 and w_2 are conditioning weights for control of the two factors. In addition, the energy flexibility of each PEV, $F_{i,t}^{PEV}$, is required for limitation of the charging operation in Fig. 4.

1) PEV'S EXISTENCE PROBABILITY BASED ENERGY ALLOCATION

Since the arrival times and the departure times of the PEV fleet are unpredictable, the operations of EVSE of the first optimization may be unused in the actual PEV charging station. Thus, the allocation priorities for EVSE operations is calculated using the probabilities of the PEVs' existence, as below:

$$\lambda_t^i = p_{i,t}^{ch} \theta_t^i p\delta_{i,t}^{ch} + p_{i,t}^{dch} \theta_t^i p\delta_{i,t}^{dch}, \quad (16)$$

where

$$p_{i,t}^{ch} = \begin{cases} \dfrac{t - t_i^{arr}}{t_i^{dep} - t_i^{arr}}, & t_i^{dep} \geq t \geq t_i^{arr} \\ 0, & \text{otherwise} \end{cases} \quad (17)$$

$$p_{i,t}^{dch} = \begin{cases} \dfrac{t_i^{dep} - t}{t_i^{dep} - t_i^{arr}}, & t_i^{dep} \geq t \geq t_i^{arr} \\ 0, & \text{otherwise} \end{cases} \quad (18)$$

$$\theta_t^i = f(x; \mu_i; \sigma_i^2), \quad \mu_i = \frac{(t_i^{dep} - t_i^{arr})}{2} \quad (19)$$

$p_{i,t}^{ch}$ and $p_{i,t}^{dch}$ are the charging and discharging weights, with the departure time showing a strong relationship to the charging priorities. Therefore, the charging controls of the PEVs terminate rapidly when charging weights are used, and the PEV departs the charging station earlier than the scheduled departure time. The θ_t^i is the probability density function of the i^{th} PEV's existence, that considers a normal distribution in the proposed method. High probabilities mean that the battery of the PEV is usable. Also, the charging/discharging amounts of each PEV is directly proportional the parking duration, since the charging operations are evenly distributed to each PEV based on the probability. In addition, the θ_t^i assumes that the standard deviation of the normal distribution increases linearly depending on the parking duration of each PEV.

2) ENERGY ALLOCATION USING THE BATTERY STATE

The battery degradation cost is based on the driving patterns of PEV owners [32]. To increase the battery lifetime, a SoC level of battery between 65%-75% of battery capacity or specific values is recommended. Thus, a SoC control factor for battery management is formulated as below:

$$b_t^i = \sum_{z=t_i^{arr}}^{t} |\kappa \times P_{i,z}^{PEV} + \psi_i^{ini} - \alpha B_i|, \quad (20)$$

where

$$P_{i,t}^{PEV} = \gamma^{ch} p\delta_{i,t}^{ch} + \gamma^{dch} p\delta_{i,t}^{dch} \quad (21)$$

$$p\delta_{i,t}^{ch} + p\delta_{i,t}^{dch} \leq 1 \quad (22)$$

z is the time index for the cumulative sum. Also, b_t^i is the distance between the SoC level at time t and α% SoC, and α is specific SoC level, that is recommended for increasing the battery lifetime. When this factor is used, the SoC of the battery is maintained around the specific SoC level during the parking duration by controlling the values of α.

3) LOAD GUIDED SIGNAL BASED CHARGING OPERATION

In the second optimization, the number of charging/discharging operations depends on the load guided signal. The number of charging operations of EVSE is equal to those of the PEVs and given below as

$$\sum_{k=1}^{N^{ch}} e\delta_{k,t}^{ch} = \sum_{i=1}^{I} p\delta_{i,t}^{ch}, \quad \forall t$$

$$\sum_{k=1}^{N^{ch}} e\delta_{k,t}^{dch} = \sum_{i=1}^{I} p\delta_{i,t}^{dch}, \quad \forall t \quad (23)$$

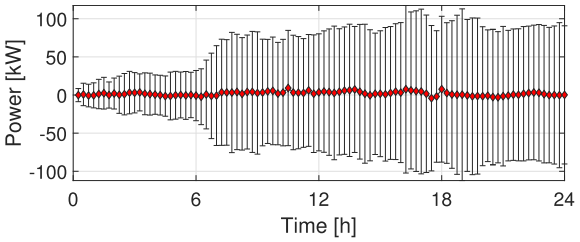

FIGURE 6. The standard deviation and the average value of energy prediction errors.

The second optimization satisfies the load guided signal, minimizing the electricity cost, and jointly considering user satisfaction.

V. NUMERICAL EVALUATION

Numerical evaluation of the performance of the proposed PEV charging coordination is based on the system model in Section II. To create the mobility model of the PEV fleet for the day-ahead scenario, the vehicle information randomly selects actual fossil-fuel vehicle entry-exit monitored data in the test period considering the penetration level. Also, the PEV multi-charger station with ±7kW charging/discharging rate is considered, and the charging/discharging efficiency parameters of EVSEs are set to $\eta_{ch} = 1.05$ and $\eta_{dch} = 0.85$. In addition, the battery cost and battery lifetime are assumed as β = 150,000 KRW and l = 10,000 cycles. To analyze the grid effects of PEV fleet, the penetration level is set to 30%, 40%, and 50%. The ratios of the three-vehicle model, including the Niro EV, IONIQ, and Soul EV, are set to 30%, 30%, 40% of the entire vehicle counts. To minimize the overall cost of the ToU tariff, the charging cost of the PEV fleet utilizes the electricity cost in Table 3, and the discharging cost of the PEV fleet considers the electricity cost for providing electricity from the PEV to the building using Table 2. The average and standard deviations of the driving distance models is considered as $\mu_d = 60$ km and $\Sigma_d = 18.22$. Finally, the contracted power, P^{ct}, is set to 755 kW by considering the average of peak load and the excessive power in the test period.

A. BUILDING LOAD PREDICTION METHOD

The energy prediction method is employed for a more practical evaluation. The time series model based linear prediction method, which is a common energy prediction model, is implemented for the day-ahead scenario. This method involves linear filter coefficients that are decided by analyzing the causality between the observed values using a reference [33]. The training data set is data from the past 1.5 years, with the test period of the load prediction for analysis of prediction errors set to 1 year. The standard deviation and the average values of the prediction error were calculated, and plotted in Fig. 6.

B. PEV CHARGING COORDINATION MODELS FOR COMPARATIVE ANALYSIS

1) FIRST COME FIRST SERVE (FCFS) CHARGING SCHEME

For comparison with the actual charging scheme, the FCFS charging scheme as introduced in [13] are employed. In the FCFS charging method, when PEVs are connected to the grid, the batteries charge promptly at the charging rates of the EVSE. The charging operations terminate when the their batteries meet the desired energy. The FCFS charging scheme is formulated as below:

$$\min_{p\delta_{i,t}^{ch}} \sum_{i=1}^{I} \sum_{t=t_i^{arr}}^{t_i^{dep}} p_{i,t}^{ch} \times p\delta_{i,t}^{ch}, \tag{24}$$

where

$$\sum_{t=t_i^{arr}}^{t_i^{dep}} (\kappa \gamma^{ch} p\delta_{t,i}^{ch}) + \psi_i^{ini} > \psi_i^{des} \tag{25}$$

2) ToU WEIGHTED COORDINATION METHOD

For intuitive evaluation, the ToU weighted coordination method introduced in reference [2] is tested. When the electricity price is high in the ToU tariff at time t, each PEV discharges the extra energy saved. The PEV freely charges and discharges within the energy flexibility of each PEVs, $F_{i,t}^{PEV}$, by considering the ToU tariff as below:

$$\min_{p\delta_{i,t}^{dch}, p\delta_{i,t}^{ch}} \sum_{i=1}^{I} \sum_{t=t_i^{arr}}^{t_i^{dep}} \kappa(\xi_t^{ch}\gamma^{ch} p\delta_{i,t}^{ch} + \xi_t^{dch}\gamma^{dch} p\delta_{i,t}^{dch}), \tag{26}$$

with constraints

$$\sum_{i=1}^{I} (p\delta_{i,t}^{dch} + p\delta_{i,t}^{ch}) < N^{ch}$$

$$\sum_{t=t_i^{arr}}^{t_i^{dep}} \kappa(\gamma^{ch} p\delta_{i,t}^{ch} - \gamma^{dch} p\delta_{i,t}^{dch}) + \psi_i^{ini} > \psi_i^{des}, \tag{27}$$

where N^{ch} is the number of the available chargers, and the number of the available chargers equals the number of PEVs in the multi-charger station environment. This method can generate a high peak load, since only the ToU tariff is considered. Also, the total benefit is reduced if the battery degradation cost is considered.

C. CASE STUDIES

The performances of three PEV charging strategies are evaluated within a week duration in summer. In the first optimization of the proposed method, the charging operations of the EVSE is controlled to minimize the overall electricity cost by considering the information of the PEV fleet. The charging operations of the EVSE in the day-ahead scenario is expressed as illustrated in Fig. 7.

The energy flexibility boundaries through the PEV fleet in the building is expressed by the black line, and the load

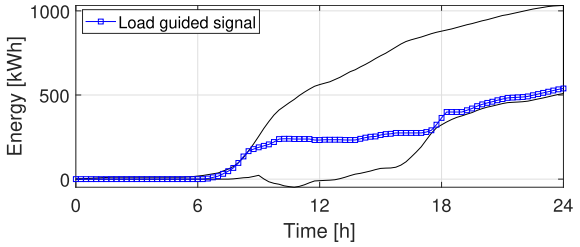

FIGURE 7. Load guided signal based on the first charging optimization.

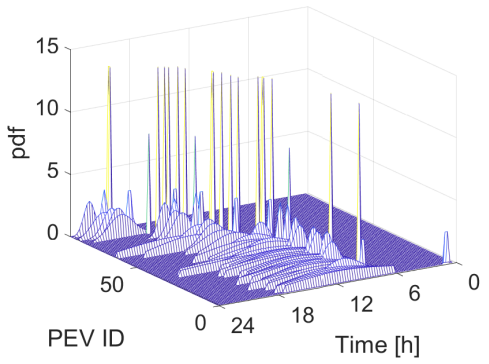

FIGURE 8. The probability density function of PEV existence based on the normal distribution with the PEV penetration level 40%.

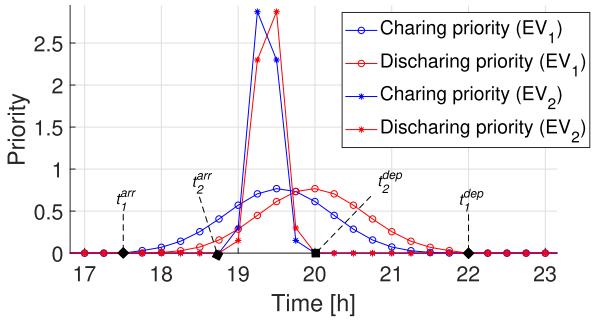

FIGURE 9. The charging/discharging priorities of two PEVs.

guided signal based on the electricity cost means the cumulative energy of the charging operations of EVSEs. The charging operation of each PEV is controlled to match the charging energy amounts of the PEV fleet to the load guided signal. To allocate the charging operations to PEVs, the probability density function of the PEV's existence is expressed as shown in Fig. 8. Since the probability density function is high value when the duration of parking is short, the PEVs with short parking periods charge their desired energy rapidly. In contrast, the PEVs with the long parking periods implement the charging strategies, when the PEVs with short parking periods are absent in the PEV charging station.

The charging/discharging priorities of two PEVs are displayed in Fig. 9. The charging priority is higher than the discharging priority near the arrival time of the PEV. This means that the charging operation usually occurs before the

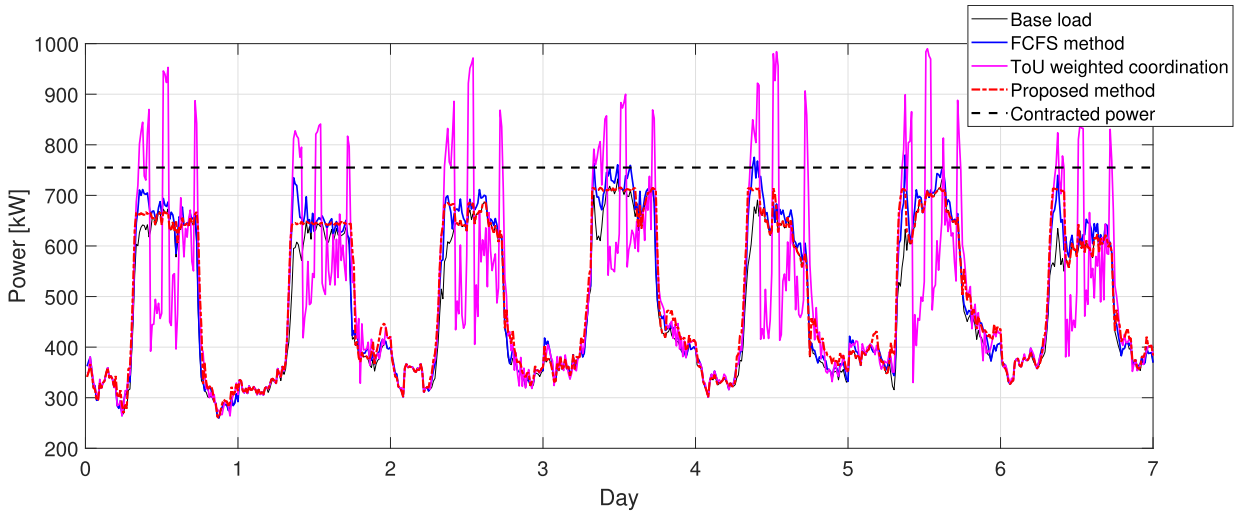

FIGURE 10. The PEV charging profiles of three PEV charging coordinations with penetration level 40%.

discharging operation, and the charging operation of most PEVs is completed quickly before departure time.

The load profiles of three charging coordination methods in the day-ahead scenario are compared in Fig. 10. In the commercial building, the FCFS method produces a high peak load in the morning, when most people are commuting. In addition, the load profile of the FCFS method is heavily influenced by the driving pattern model of the PEV fleet, because the maximum peak load appears when the arriving number of PEVs is high. Thus, the maximum peak load is generated in the morning if the number of F type and M type vehicles increases. The ToU weighted coordination is shown in the the magenta line in Fig. 10. In the ToU weighted coordination, high fluctuation of power emerges depending on the ToU tariff, with the power overload generated because all PEVs charge at low-price timezone. Conversely, the proposed method is represented by the dotted red line, providing low peak power and low fluctuation because the demand cost of the contracted power and the ToU tariff are considered jointly. The baseline cost is paid monthly the contracted power. In the proposed method, the new contracted power is decided from the highest value of the power profiles in the simulation period. If the maximum peak load occurs on the previous day, the batteries of the PEVs in following day are charged and discharged using the ToU tariff by configuring new contracted power based on the maximum peak power of the previous days. In the fourth day in Fig. 10, the charging operations of the proposed method is based on the ToU tariff under a new contracted power.

The cost performances of these charging coordination methods are evaluated, as illustrated in Fig. 11. This result shows the average values of the costs and the standard deviations of costs from 10 tests. The baseline cost of the proposed method is the lowest value, since the maximum peak power is reduced. However, the battery degradation cost and charging/discharging loss cost is higher than for the FCFS method, since much energy is used to reduce the maximum peak load. On the other hand, the ToU weighted coordination generates high penalty cost and high battery degradation cost, and the overall cost is about 40% higher than for the FCFS method. In addition, the ToU tariff weighted coordination pays additional cost, because the battery degradation cost and the contracted power are not considered. In terms of the battery degradation cost, the FCFS method has the best solution, because the charging operations of the PEV fleet meet only to the desired energy, but it generates a high peak load in the building at morning time. Consequently, the overall cost of the proposed method is about 7% better than FCFS method in penetration level 40%.

In this study, the stability of the power system by PEV fleet is analyzed. The load factor is obtained by accounting for the base load of the building and the charging energies of PEVs, as follows:

$$\text{Load factor} = \frac{\sum_{t=1}^{T}(P_t^B + \sum_{k=1}^{N^{ch}} P_{k,t}^{EVSE})}{\max(P_t^B + \sum_{k=1}^{N^{ch}} P_{k,t}^{EVSE})} \times \frac{100}{T}[\%] \quad (28)$$

The load factor is an indicator of whether the power equipment is operating efficiently. As the load factor approaches 100%, it means that the power equipment is used efficiently. The load factors of the building according to the charging strategies are compared in Fig. 12. It is confirms that the FCFS method and the ToU weighted coordination increase the maximum peak load, and lower the load factors. In contrast, since the maximum peak load of the proposed method is lower than base load, this stabilizes the power system. With a penetration level of 40%, the load factor of the proposed method improves by about 9% relative to that of the FCFS scheme with the results analyzed in Fig. 13.

The performance improvement rate means the degree of improvement when the proposed method is compared with the FCFS method. As the number of PEVs increases,

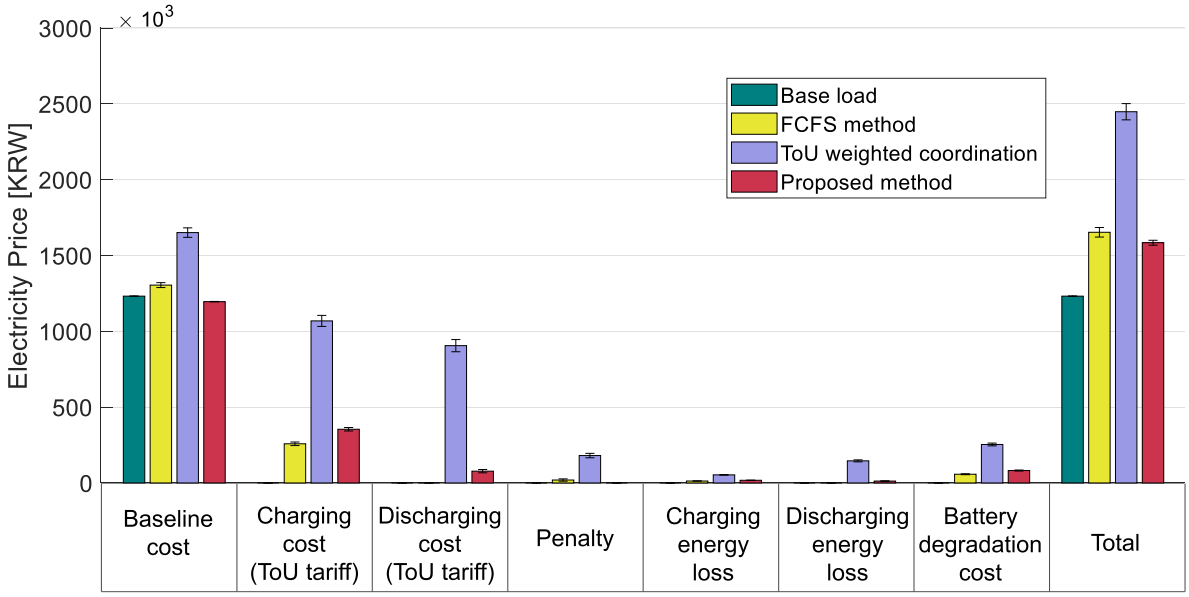

FIGURE 11. The cost performances of three charging strategies with the PEV penetration level 40%.

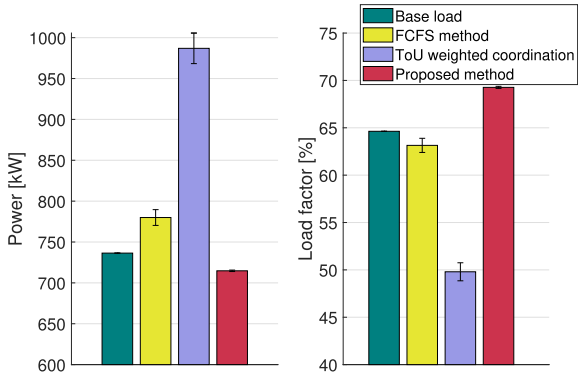

FIGURE 12. The impact of the three charging strategies with penetration level 40%, (left) the maximum peak load, and (right) the load factor on power system.

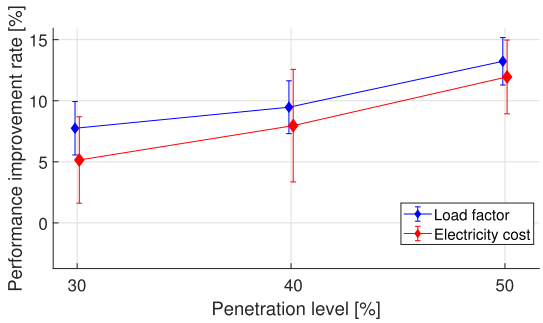

FIGURE 13. Performance improvement rate of the proposed charging coordination by penetration level.

the energy required by PEVs also rises. Thus, the FCFS method generates a higher peak load and high overall costs. Conversely, the proposed method offers more positive effects for the building's energy system, because the building energy system has lots of available energy at high penetration level. Thus, the performance improvement rate is improved, as the penetration level increases, as described in Fig. 13. In addition, since the driving patterns of the PEV fleet are created randomly, the variation of results exists. If the parking duration of most PEVs is short, the energy flexibilities of the PEV fleet is reduced. As the result, the driving pattern models of the PEV fleet affects the performance of the proposed method.

In our proposed system, the performances using the prediction error are evaluated in order to consider the actual environment. To evaluate the performance, the building load profile are used through the load prediction instead of actual load profile, as below:

$$P_t^B = \hat{P}_t^B + w_3 \sigma_t^{pred}, \tag{29}$$

where σ_t^{pred} is the standard deviation of prediction errors at time t as shown in Fig. 6, and w_3 is the conditioning weight, which acts as the buffer of the prediction error. In the proposed method, when the prediction error is quite large, its buffer suppresses the charging amount of the PEV fleet to lower the contracted power. Instead, the overall cost performance may decrease, and the load factor and cost performances by the prediction errors are described in Fig. 14. The load prediction error is calculated using the mean absolute percentage error (MAPE). As the prediction error increases, the performance improvement rate is reduced dramatically in Fig. 14. When $w_3 = 1$ or 2, the performances of cost and load factor is compensated. However, the cost performance of the proposed method is lower than the FCFS method if MAPE is 5.5%, although the buffer is used. To apply the

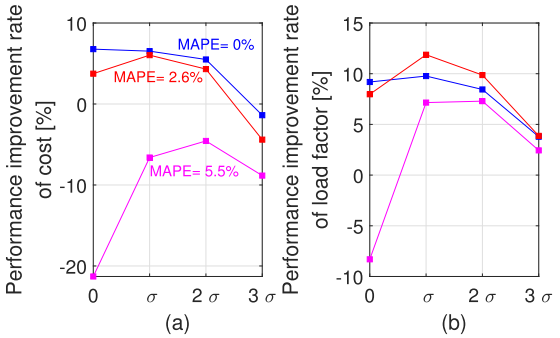

FIGURE 14. Performance improvement rate of PEV charging coordination based on load prediction of building with penetration level 50%.

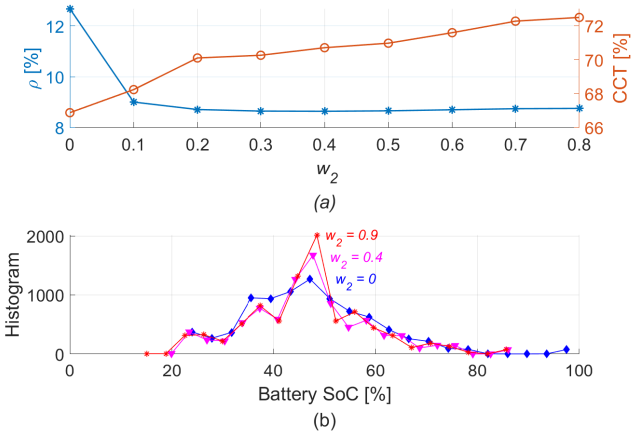

FIGURE 15. The battery performance of PEVs by w_2 for PEV owner. (a) the average SoC of PEVs and the charging completion time. (b) the histogram of battery SoCs.

proposed method, the prediction, showing a high performance is needed.

In this study, the user satisfaction is also evaluated. The previous methods for V2B does not consider the variation of the SoC levels of PEVs. To improve the lifetime of the battery, the SoCs of PEVs must stay within a certain range. For the evaluation of the battery states, the ρ factor for battery lifetime is defined as below:

$$\rho = \frac{1}{\sum_{t=1}^{T} N_t^{PEV}} \sum_{i=1}^{I} \sum_{t=t_i^{arr}}^{t_i^{dep}} \frac{b_t^i}{B_i} \times 100[\%], \qquad (30)$$

where ρ is the average of the distances between $\alpha\%$ and SoC levels of the PEV fleet. The α configures 50% in the day-ahead scenario, and as w_2 increases, it is shown that many PEVs proceed charging operations near 50%, as illustrated in Fig. 15(a) and (b). The performance of ρ improves as the w_2 increases. However, the performance of rho converges specific value when w_2 is larger than 0.3 because each PEV should satisfy the departing SoC level.

In addition, the charging completion time (CCT) is evaluated as the user satisfaction values. If the charging operations of the PEV fleet quickly ends, the variation of the PEV's departure time does not affect the PEV charging coordination method. Therefore, the CCT is an essential factor for the evaluation of the user satisfaction, and is formulated as:

$$\text{CCT} = \sum_{i=1}^{I} \left(\frac{\max((t - t_i^{arr}) \times p\delta_{i,t}^{ch})}{t_i^{dep} - t_i^{arr}} \right) \times \frac{100}{I}[\%] \qquad (31)$$

A low CCT value implies the charging operation of most PEVs ends quickly. The charging operation of PEVs finishes rapidly before the departure time if only the probability density function of PEV's existence is considered ($w_2 = 0$). As w_2 increases, the charging complete time rises, as displayed in Fig. 15(a). Thus, w_1 and w_2 require proper control considering the effects of battery and CCT.

VI. CONCLUSION

This study introduces a novel PEV charging coordination scheme for flexible charging/discharging operations of the PEV fleet by considering the energy cost of the building as well as the PEV requirements. The proposed method consists of two optimization processes with separate objective functions. The first optimization minimizes overall energy cost of the building by controlling the operations of the EVSE in the PEV charging station of the building, while limiting the impact on the stability of the building's energy system. In this step, all cost constraints are jointly considered like the ToU tariff, contracted power, and battery degradation costs. In the second optimization, the satisfaction of PEV owners is the primary concern, and it is improved by prioritizing the charging demands of the PEVs by the probability density function of their existence and SoC levels of their batteries. For evaluations, the impacts of the load prediction error and penetration level on the performances of both the electricity cost and the load factor are investigated. The results of case studies are summarized:

- The cost benefit of the PEV fleet in smart building is generated from the reduction of the demand charge cost mainly. The proposed method could provide 12% cost reduction and 13% load factor increase with penetration level of 50%. For the power system, the proposed method contributes in stabilizing the building's energy system, since the peak power is reduced by utilizing the available energy of the PEV fleet.
- For the PEV's owner, the user satisfaction is improved by completing the charging request of PEV quickly. Also, the lifetime of the battery is improved by carefully controlling the priority of the PEVs.

REFERENCES

[1] *Global EV Outlook 2016: Beyond One Million Electric Cars*, Int. Energy Agency, Paris, France, 2016, pp. 29–37.
[2] S. Yoon, K. Park, and E. Hwang, "Connected electric vehicles for flexible vehicle-to-grid (V2G) services," in *Proc. Int. Conf. Inf. Netw. (ICOIN)*, Jan. 2017, pp. 411–413.
[3] J. A. P. Lopes, F. J. Soares, and P. M. R. Almeida, "Integration of electric vehicles in the electric power system," *Proc. IEEE*, vol. 99, no. 1, pp. 168–183, Jan. 2011.

[4] R.-C. Leou, C.-L. Su, and C.-N. Lu, "Stochastic analyses of electric vehicle charging impacts on distribution network," *IEEE Trans. Power Syst.*, vol. 29, no. 3, pp. 1055–1063, May 2014.
[5] K. Mahmud, M. J. Hossain, and G. E. Town, "Peak-load reduction by coordinated response of photovoltaics, battery storage, and electric vehicles," *IEEE Access*, vol. 6, pp. 29353–29365, 2018.
[6] M. L. Crow, "Cost-constrained dynamic optimal electric vehicle charging," *IEEE Trans. Sustain. Energy*, vol. 8, no. 2, pp. 716–724, Oct. 2017.
[7] M. C. Kisacikoglu, F. Erden, and N. Erdogan, "Distributed control of PEV charging based on energy demand forecast," *IEEE Trans. Ind. Informat.*, vol. 14, no. 1, pp. 332–341, Jan. 2018.
[8] L. Cheng, Y. Chang, and R. Huang, "Mitigating voltage problem in distribution system with distributed solar generation using electric vehicles," *IEEE Trans. Sustain. Energy*, vol. 6, no. 4, pp. 1475–1484, Oct. 2015.
[9] J. García-Villalobos, I. Zamora, J. I. S. Martín, I. Junquera, and P. Eguía, "Delivering energy from PEV batteries: V2G, V2B and V2H approaches," in *Proc. Int. Conf. Renew. Energies Power Qual. (ICREPQ)*, La Coruña, Spain, 2015, pp. 215–247.
[10] R. D'hulst, W. Labeeuw, B. Beusen, S. Claessens, G. Deconinck, and K. Vanthournout, "Demand response flexibility and flexibility potential of residential smart appliances: Experiences from large pilot test in Belgium," *Appl. Energy*, vol. 155, pp. 79–90, Oct. 2015.
[11] A. Schuller, B. Dietz, C. M. Flath, and C. Weinhardt, "Charging strategies for battery electric vehicles: Economic benchmark and V2G potential," *IEEE Trans. Power Syst.*, vol. 29, no. 5, pp. 2014–2022, Sep. 2014.
[12] P. Y. Kong and G. K. Karagiannidis, "Charging schemes for plug-in hybrid electric vehicles in smart grid: A survey," *IEEE Access*, vol. 4, pp. 6846–6875, Nov. 2016.
[13] S. Yoon and E. Hwang, "Poster: Electric vehicle network bidirectional charging for flexible vehicle-to-grid services," in *Proc. IEEE Veh. Netw. Conf. (VNC)*, Dec. 2016, pp. 1–2.
[14] M. Ghofrani, A. Arabali, M. Etezadi-Amoli, and M. S. Fadali, "Smart scheduling and cost-benefit analysis of grid-enabled electric vehicles for wind power integration," *IEEE Trans. Smart Grid*, vol. 5, no. 5, pp. 2306–2313, Sep. 2014.
[15] H. N. T. Nguyen, C. Zhang, and M. A. Mahmud, "Optimal coordination of G2V and V2G to support power grids with high penetration of renewable energy," *IEEE Trans. Transport. Electrific.*, vol. 1, no. 2, pp. 188–195, Aug. 2015.
[16] S. Xie, W. Zhong, K. Xie, R. Yu, and Y. Zhang, "Fair energy scheduling for vehicle-to-grid networks using adaptive dynamic programming," *IEEE Trans. Neural Netw. Learn. Syst.*, vol. 27, no. 8, pp. 1697–1707, Aug. 2016.
[17] K. Park, S. Yoon, and E. Hwang, "Flexible charging coordination for plug-in electric vehicles based on uniform stochastic charging demand and time-of-use tariff," in *Proc. IEEE Transp. Electrific. Conf. Expo (ITEC)*, 2019, pp. 1–4.
[18] A. E. P. Abas, J. Yong, T. M. I. Mahlia, and M. A. Hannan, "Techno-economic analysis and environmental impact of electric vehicle," *IEEE Access*, vol. 7, pp. 98565–98578, 2019.
[19] J. Neubauer and M. Simpson, "Deployment of behind-the-meter energy storage for demand charge reduction," Nat. Renew. Energy Lab., Lakewood, CO, USA, Tech. Rep. NREL/TP-5400-63162, 2015.
[20] D. Park, S. Yoon, and E. Hwang, "Cost benefit analysis of public service electric vehicles with vehicle-to-grid (V2G) capability," in *Proc. IEEE Conf. Expo Transp. Electrific. Asia–Pacific (ITEC Asia–Pacific)*, Jun. 2016, pp. 234–239.
[21] L. Noel and R. McCormack, "A cost benefit analysis of a V2G-capable electric school bus compared to a traditional diesel school bus," *Appl. Energy*, vol. 126, pp. 246–255, Aug. 2014.
[22] M. Shafie-khah, E. Heydarian-Forushani, G. J. Osório, F. A. Gil, J. Aghaei, M. Barani, and J. P. S. Catalão, "Optimal behavior of electric vehicle parking lots as demand response aggregation agents," *IEEE Trans. Smart Grid*, vol. 7, no. 6, pp. 2654–2665, Nov. 2016.
[23] S. Yoon and E. Hwang, "Electric vehicle fleet model based cooperative charging coordination for medium-sized smart buildings," in *Proc. 2nd Int. Conf. Electr. Vehicle, Smart Grid Inf. Technol. (ICESI)*, 2017, pp. 287–290.
[24] M. R. Sarker, M. A. Ortega-Vazquez, and D. S. Kirschen, "Optimal coordination and scheduling of demand response via monetary incentives," *IEEE Trans. Smart Grid*, vol. 6, no. 3, pp. 1341–1352, May 2015.
[25] O. Erdinc, N. G. Paterakis, T. D. P. Mendes, A. G. Bakirtzis, and J. P. S. Catalão, "Smart household operation considering bi-directional EV and ESS utilization by real-time pricing-based DR," *IEEE Trans. Smart Grid*, vol. 6, no. 3, pp. 1281–1291, May 2015.
[26] Z. Fan, "A distributed demand response algorithm and its application to PHEV charging in smart grids," *IEEE Trans. Smart Grid*, vol. 3, no. 3, pp. 1280–1290, Sep. 2012.
[27] N. Neyestani, M. Y. Damavandi, M. Shafie-Khah, A. G. Bakirtzis, and J. P. S. Catalão, "Plug-in electric vehicles parking lot equilibria with energy and reserve markets," *IEEE Trans. Power Syst.*, vol. 32, no. 3, pp. 2001–2016, Sep. 2017.
[28] M. Shafie-Khah, P. Siano, D. Z. Fitiwi, N. Mahmoudi, and J. P. S. Catalão, "An innovative two-level model for electric vehicle parking lots in distribution systems with renewable energy," *IEEE Trans. Smart Grid*, vol. 9, no. 2, pp. 1506–1520, Mar. 2018.
[29] H. Nafisi, S. M. M. Agah, H. A. Abyaneh, and M. Abedi, "Two-stage optimization method for energy loss minimization in microgrid based on smart power management scheme of PHEVs," *IEEE Trans. Smart Grid*, vol. 7, no. 3, pp. 1268–1276, May 2016.
[30] D. T. Hoang, P. Wang, D. Niyato, and E. Hossain, "Charging and discharging of plug-in electric vehicles (PEVs) in vehicle-to-grid (V2G) systems: A cyber insurance-based model," *IEEE Access*, vol. 5, pp. 732–754, 2017.
[31] S. Yoon, K. Park, and E. Hwang, "Vehicle-to-building availability analysis based on the flexible building guide and the vehicle fleet modeling associated with the building category," *KIISE Trans. Comput. Pract.*, vol. 24, no. 11, pp. 582–588, 2018.
[32] B. Xu, A. Oudalov, A. Ulbig, G. Andersson, and D. S. Kirschen, "Modeling of lithium-ion battery degradation for cell life assessment," *IEEE Trans. Smart Grid*, vol. 9, no. 2, pp. 1131–1140, Mar. 2018.
[33] K. Park, S. Yoon, and E. Hwang, "Hybrid load forecasting for mixed-use complex based on the characteristic load decomposition by pilot signals," *IEEE Access*, vol. 7, pp. 12297–12306, 2019.

SEUNGWOOK YOON received the B.S. degree from the Department of Electric Engineering, Kwangwoon University, Seoul, South Korea, in 2014. He is currently pursuing the integrated M.S. and Ph.D. degrees with the School of Mechatronics, Gwangju Institute of Science and Technology, Gwangju, South Korea. His research interests include energy informatics, vehicle grid integration, and data channel array signal processing.

EUISEOK HWANG received the B.S. and M.S. degrees from the School of Engineering, Seoul National University, Seoul, South Korea, in 1998 and 2000, respectively, and the M.S. and Ph.D. degrees in electrical and computer engineering from Carnegie Mellon University, Pittsburgh, PA, USA, in 2010 and 2011, respectively. He was with the Digital Media Research Center, Daewoo Electronics Company Ltd., South Korea, from 2000 to 2006, and was with the Channel Architecture Group, LSI Corporation (now Broadcom), San Jose, CA, USA, from 2011 to 2014. Since 2015, he has been an Assistant/Associate Professor with the School of Mechatronics, Gwangju Institute of Science and Technology, South Korea. He holds 21 granted U.S. patents. He has over 100 journals and conference papers in information and signal processing issues. His research interests include signal disaggregation, equalization, and coding for data communication channels and emerging large-scale information processing applications, such as smart grids.